Local accumbens in vivo imaging during deep brain stimulation reveals a strategy-dependent amelioration of hedonic feeding

Hemmings Wu[a,1], Bina Kakusa[a,1], Sophie Neuner[a,b], Daniel J. Christoffel[b], Boris D. Heifets[c], Robert C. Malenka[b], and Casey H. Halpern[a,d,2]

[a]Department of Neurosurgery, Stanford University School of Medicine, Stanford, CA 94305; [b]Nancy Pritzker Laboratory, Department of Psychiatry and Behavioral Science, Stanford University School of Medicine, Stanford, CA 94305; [c]Department of Anesthesiology, Perioperative and Pain Medicine, Stanford University School of Medicine, Stanford, CA 94305; and [d]Richards Medical Research Laboratories, Department of Neurosurgery, Perelman School of Medicine at the University of Pennsylvania, Philadelphia, PA 19104

Edited by Donald Pfaff, Laboratory of Neurobiology and Behavior, Rockefeller University, New York, NY; received May 19, 2021; accepted October 28, 2021

Impulsive overeating is a common, disabling feature of eating disorders. Both continuous deep brain stimulation (DBS) and responsive DBS, which limits current delivery to pathological brain states, have emerged as potential therapies. We used in vivo fiber photometry in wild-type, Drd1-cre, and A2a-cre mice to 1) assay subtype-specific medium spiny neuron (MSN) activity of the nucleus accumbens (NAc) during hedonic feeding of high-fat food, and 2) examine DBS strategy-specific effects on NAc activity. D1, but not D2, NAc GCaMP activity increased immediately prior to high-fat food approach. Responsive DBS triggered a GCaMP surge throughout the stimulation period and durably reduced high-fat intake. However, with continuous DBS, this surge decayed, and high-fat intake reemerged. Our results argue for a stimulation strategy-dependent modulation of D1 MSNs with a more sustained decrease in consumption with responsive DBS. This study illustrates the important role in vivo imaging can play in understanding effects of such novel therapies.

responsive neurostimulation | deep brain stimulation | fiber photometry | hedonic feeding | nucleus accumbens

Approximately one-third of individuals afflicted with eating disorders remain treatment-refractory to both pharmacologic interventions and psychotherapy (1, 2). A defining characteristic of most eating disorders is overeating behavior that can be the most disabling and difficult-to-treat feature. Moreover, over 30% of the US population is obese amid a worldwide epidemic. Up to 50% of obese individuals exhibit periods of uncontrolled overeating that is pervasive among *Diagnostic and Statistical Manual of Mental Disorders*, Fifth Edition–defined eating disorders, with binge eating disorder as the most common of these disorders (3–6). The nucleus accumbens (NAc) is thought to mediate hedonic feeding by integrating limbic inputs for affective processing and cue-triggered motivation, as well as cortical inputs for action selection (7, 8). Not surprisingly, when the mesocorticolimbic circuit involving the NAc is perturbed, hedonic feeding behaviors can present more prominently (9, 10). This perturbation may have cell-type specificity within the NAc, as it has been reported that selective dopamine D1 receptor–expressing medium spiny neuron (MSN) activation promotes cocaine place preference, enhances cocaine seeking in response to contextual cues, prevents extinction, and facilitates reinstatement (11, 12). Moreover, a subpopulation of D1 MSNs has been reported to provide the predominant NAc inhibitory output to the lateral hypothalamus and to receive the bulk of afferent projections from the lateral hypothalamus, further resolving a circuit that may override homeostatic need (13).

Preclinical and rare clinical studies have reported that "open-loop" or continuous deep brain stimulation (cDBS) of the NAc attenuates hedonic feeding and other reward-seeking behaviors (14–17), including binge-like alcohol drinking (18). Subsequent efforts to deliver episodic, "closed-loop" or responsive DBS (rDBS) guided by peaks in delta-range field potentials revealed equivalent if not superior amelioration in overconsumption with significantly less current delivery and fewer adverse effects (19). Further, rDBS could provide a means for adaptive, automated programming via biofeedback algorithms to optimize stimulation parameters to subject-specific differences (20–22). Nevertheless, we have a poor understanding of the underlying therapeutic mechanisms of DBS and the interaction between DBS and its targeted pathophysiology, which stifles the future success of a closed-loop intervention.

A critical reason these mechanisms elude our understanding is the limited ability to simultaneously record neuronal population activity during DBS (23, 24). Calcium imaging using fiber photometry has emerged as an in vivo methodology to measure

Significance

Impulsive overeating is a common, disabling feature of eating disorders. Calcium imaging using fiber photometry has emerged as an in vivo methodology to measure neuronal population activity immune to electrical stimulation artifact from deep brain stimulation (DBS). Thus, when used simultaneously, calcium imaging can elucidate poorly understood DBS mechanisms. We show that nucleus accumbens D1 medial spiny calcium signaling increases in preparation of hedonic feeding of high-fat food. Further, responsive, over continuous, DBS strategies effectively disrupt this activity leading to decreased consumption. Implementation of this methodology to better understand mechanisms of these and other forms of neuromodulation for various indications may help advance the field to identify novel therapeutic targets with applications extending beyond obesity.

Author contributions: H.W., B.K., D.J.C., B.D.H., R.C.M., and C.H.H. designed research; H.W., B.K., and S.N. performed research; H.W., B.K., S.N., D.J.C., B.D.H., R.C.M., and C.H.H. contributed new reagents/analytic tools; H.W., B.K., and S.N. analyzed data; and H.W., B.K., D.J.C., B.D.H., R.C.M., and C.H.H. wrote the paper.

Competing interest statement: C.H.H. actively consults for Boston Scientific and Ad-Tech. H.W., R.C.M., and C.H.H. have an invention on the delta band (WO2018064225) filed September 2017, reflecting loss of control behaviors, but no commercial interest owns this patent.

This article is a PNAS Direct Submission.

[1]H.W. and B.K. contributed equally to this work.

[2]To whom correspondence may be addressed. Email: casey.halpern@pennmedicine.upenn.edu.

This article contains supporting information online at http://www.pnas.org/lookup/suppl/doi:10.1073/pnas.2109269118/-/DCSupplemental.

Published December 17, 2021.

neuronal population activity immune to electrical stimulation artifact (25). Here, we first use fiber photometry to examine local activity in the NAc before and after stable hedonic feeding behavior is developed in mice using a limited exposure to a high-fat (HF) food protocol. We then carried out simultaneous NAc fiber photometry during cDBS and rDBS to examine potential physiologic dissociations in ameliorating hedonic feeding.

Results

Parallel Increases in Hedonic Feeding Behavior and NAc Activity. First, we investigated overall NAc activity during hedonic feeding behavior by expressing GCaMP6f (AAV-DJ serotype, concentration 10^{12} to 10^{13} gc/ml) in the NAc and recording GCaMP signals in sated mice given limited access to HF food (Fig. 1 *A–D*). The calcium fluorescence signal surrounding these HF approach time frames was extracted to calculate the fractional fluorescence response (GCaMP signal or d*F*/*F*). HF intake was significantly increased in mice after developing hedonic feeding behavior with 10 d of limited HF exposure as expected (Fig. 1*E*; intake day 10 vs. day 1: $t = 5.979$, $P = 0.0019$). The NAc MSN GCaMP signal was increased during HF approach on day 10 compared with day 1, but not during locomotion unrelated to HF approach (Fig. 1 *F–H*; HF approach d*F*/*F* day 10 vs. day 1: $t = 2.942$, $P = 0.0084$; HF-unrelated locomotion d*F*/*F* day 10 vs. day 1: $t = 0.08828$, $P = 0.9305$).

Hedonic Feeding Behavior Correlates with Activity of NAc D1 MSNs Only. We explored D1 and D2 MSN-specific activity before and after developing hedonic feeding behavior using cell type–specific GCaMP signal in Drd1-cre (Fig. 2 *A–C*). Significantly increased GCaMP signals were found in Drd1-cre mice during HF approach after they developed hedonic feeding behavior, but not during HF-unrelated locomotion (Fig. 2 *C–F*; HF intake day 10 vs. day 1: $t = 13.04$, $P < 0.0001$; HF approach d*F*/*F* day 10 vs. day 1: $t = 4.317$, $P = 0.0015$; HF-unrelated locomotion day 10 vs. day 1: $t = 0.9526$, $P = 0.3632$). These changes were not found in A2a-cre mice during HF approach (Fig. 3 *A–C*), suggesting specific D1, but not D2, MSN activation occurred before and during bouts of stable HF intake (Fig. 3 *C–F*; HF intake day 10 vs. day 1: $t = 18.66$, $P < 0.0001$; HF approach d*F*/*F*: day 10 vs. day 1: $t = 0.9878$, $P = 0.3351$; HF-unrelated locomotion day 10 vs. day 1: $t = 0.1382$, $P = 0.89$). We considered whether the absence of HF approach-related transients in D2 MSNs could be attributed to insufficient GCaMP signal; however, we found comparable variation of the fluorescence signal in both D1-cre and A2a-cre groups (Fig. 3 *G* and *H*).

Fiber Photometry Dissociates the Physiologic Basis of Hedonic Feeding Attenuation by NAc cDBS and rDBS. To assess for potential electrical artifact and the threshold at which NAc activity emerged, we first applied cDBS at low frequency (i.e., delta range) and recorded NAc GCaMP signal response in an open-field test. cDBS at 3 Hz did not elicit GCaMP signal despite increased current amplitude (Fig. 4*A*). We then tested cDBS at 130 Hz, a frequency previously found to block hedonic feeding in mice, and commonly used in human neuropsychiatric applications (19). With an hour of 130-Hz cDBS (cDBS-1h), we observed a time- and dose-dependent effect on NAc MSNs with a large and more immediate ramp up of GCaMP signal persisting for the first minute and returning to baseline for the rest of the DBS period (Fig. 4*B* and *SI Appendix*, Fig. S1*A*).

Next, we recorded MSN GCaMP signal with simultaneous 3- or 130-Hz cDBS in the NAc in mice with limited exposure to HF food (Fig. 4*C*). As previously reported, cDBS at 130 Hz blocked hedonic feeding behavior, while 3-Hz cDBS had no detectable effect (Fig. 4*D*; HF intake with cDBS at 130 vs. 3 Hz vs. off: $F = 74.18$, $P < 0.0001$; post hoc: 130 Hz vs. cDBS-off: $P < 0.0001$; 130 vs. 3 Hz: $P = 0.0012$; 3 Hz vs. cDBS-off: $P = 0.58$; Tukey's correction applied). These behavioral effects were paralleled by significantly lower HF-linked GCaMP transients within the NAc during HF approach under 130-Hz cDBS-1h, while these transients were unaffected by 3-Hz cDBS as with cDBS turned off (Fig. 4 *E* and *F*; HF approach d*F*/*F*: 130 vs. 3 Hz vs. cDBS-off, $F = 3.181$, $P = 0.0427$; post hoc: 130 Hz vs. cDBS-off: $P = 0.0342$; 130 vs. 3 Hz: $P = 0.13$; 3 Hz vs. off: $P = 0.74$; Tukey's correction applied).

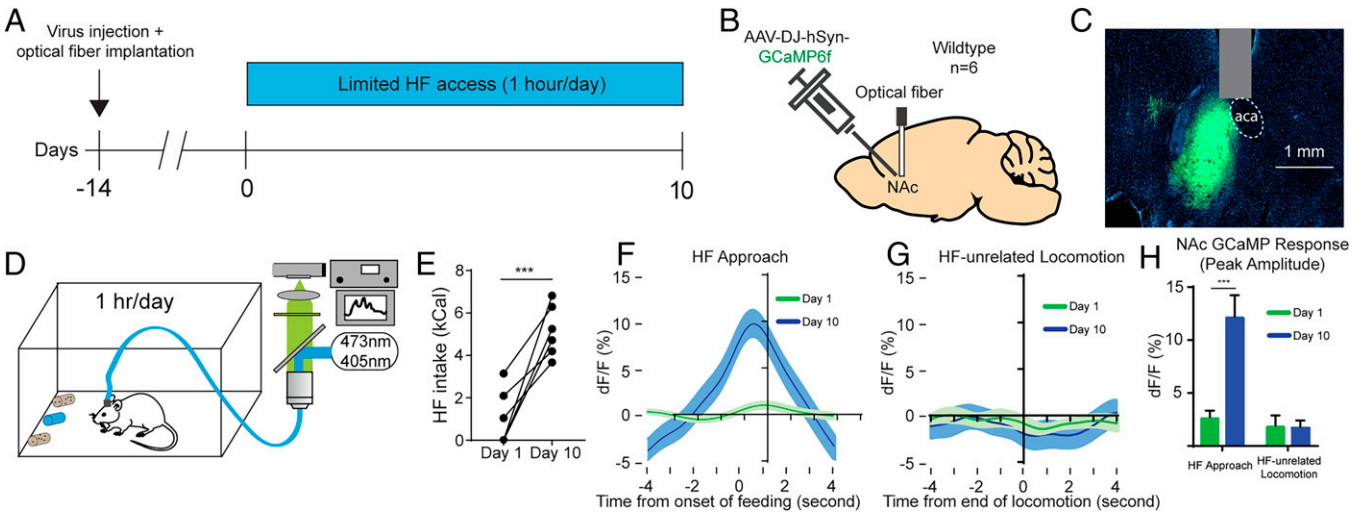

Fig. 1. NAc MSN population activity during limited exposure to HF food. (*A*) Schematic of the experimental design: virus injection and electrode implantation, followed by a recovery period (14 d) and limited HF access (days 1 to 10). (*B*) AAV-DJ-hSyn-GCaMP6f was injected into the NAc, followed by implantation of a 430-μm optical fiber in the NAc to allow for measurement of GCaMP6f signals. (*C*) Representative image of GCaMP6f expression and fiber optic implant in the NAc. (*D*) Schematic of the fiber photometry configuration and behavioral setup. (*E*) Hedonic feeding behavior developed and stabilized by day 10 of limited HF exposure (1 h/d), indicated by a significant increase in daily HF intake. (*F–H*) Average traces and quantification of the peak amplitude of the Ca^{2+} signal from the NAc in the 8-s window during HF food approach and locomotion unrelated to HF food on days 1 and 10. Data represent mean ± SEM. ***$P < 0.001$.

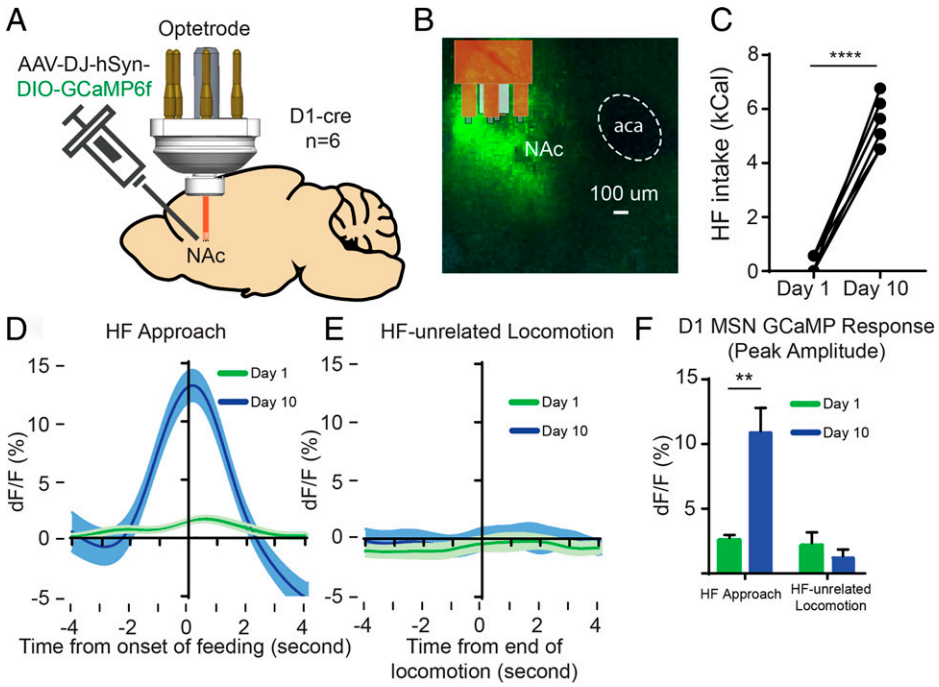

Fig. 2. NAc D1-MSN GCaMP response during hedonic feeding. (*A*) AAV-DJ-hSyn-DIO-GCaMP6f was injected into the NAc in D1-cre mice, followed by implantation of an optetrode, to allow for measurement of GCaMP6f signals in D1 MSNs. (*B*) Representative image of GCaMP6f expression in D1 MSNs and the optetrode implant in the NAc. (*C*) Hedonic feeding behavior developed and stabilized by day 10 (1 h/d), indicated by a significant increase in daily HF intake. (*D–F*) Average traces and quantification of the peak amplitude of the GCaMP fluorescence signal from the D1 MSN in the NAc in the 8-s window during HF food approach and locomotion unrelated to HF food on days 1 and 10. Data represent mean ± SEM. $^{**}P < 0.01$, $^{****}P < 0.0001$.

To investigate the durability of this effect on the GCaMP signal, we initiated cDBS at 130 Hz for 3 h prior to and during the 1-h HF exposure (cDBS-3h; Fig. 5*A*). During this assay, HF exposure was initiated hours after DBS was turned on to approximate how cDBS is used in human subjects. Given prior data suggesting loss of effect over time in more chronic studies, efficacy assessments of hedonic feeding amelioration with DBS activation irrespective of the timing of HF exposure were of interest (14). With cDBS-3h, as with cDBS-1h, both HF intake and the HF-linked GCaMP signal were decreased compared with cDBS-off (Fig. 5 *B–D*). However, during cDBS-3h, there was a relative increase in HF intake and the GCaMP signal trended toward an increase compared with during cDBS-1h (Fig. 5 *B–D*; HF intake: cDBS-3h vs. cDBS-1h, DBS-1h vs. DBS-off: $F = 55.85$, $P < 0.0001$; post hoc: cDBS-3h vs. cDBS-1h: $P = 0.031$; cDBS-3h vs. DBS-off: $P = 0.0017$; cDBS-1h vs. cDBS-off: $P = 0.0006$; HF approach-related dF/F cDBS-3h vs. cDBS-1h vs. DBS-off: $F = 11.88$, $P < 0.0001$; post hoc: cDBS-3h vs. cDBS-1h: $P = 0.44$; cDBS-3h vs. DBS-off: $P < 0.0070$; cDBS-1h vs. DBS-off: $P < 0.0001$). We considered the possibility that a generalized change in GCaMP sensitivity associated with DBS could explain the observed decrease in the HF-linked GCaMP signal with cDBS at 130 Hz. We found comparable variation of the fluorescence signal, as a proxy for detectable spontaneous activity, between DBS-off, cDBS-1h, and cDBS-3h (*SI Appendix*, Fig. S1 *A*, *Inset* and *B*).

We previously demonstrated that rDBS guided by the delta band effectively blocks hedonic feeding behavior in mice (19). Here, we observed that each bout of stimulation, which was programmed to initiate on detection of a 20% increase in delta-band power and to last 10 s, led to consistent, massive spikes in GCaMP signal, similar to the initial phase of cDBS (*SI Appendix*, Fig. S1 *C* and *D*). These signal increases returned to baseline range immediately after stimulation was stopped. Here again, rDBS significantly blocked hedonic feeding in mice when initiated 1-h and 3-h prior to HF exposure (rDBS-1h and rDBS-3h, respectively), and its effects on hedonic feeding and GCaMP signal were sustained (Fig. 5 *E–G*; HF intake: rDBS-3h vs. rDBS-1h vs. rDBS-off, $F = 81.06$, $P < 0.0001$; post hoc: rDBS-3h vs. rDBS-1h: $P = 0.68$; rDBS-3h vs. off: $P = 0.0002$; rDBS-1h vs. off: $P = 0.0003$; rDBS success rate: rDBS-3h: 78.2 ± 11.0%; rDBS-1h: 82.8 ± 5.2%; $t = 0.08619$, $P = 0.93$). During this 3-h period, a total of 698 rDBS stimulation bouts were triggered across all six mice, for an average of 19.4 min of cumulative stimulation per mouse. The average numbers of rDBS stimulation bouts during 1-h HF exposure and 3 h prior without HF exposure were 74.83 ± 17.53 and 45.33 ± 9.83, respectively (Fig. 5*H*; 29.00 ± 5.29 for the first hour and 16.33 ± 4.67 for the second hour). Therefore, rDBS remained durably effective even while delivering stimulation for only 10.7% of the recorded 3-h period and 20.8% of the 1-h period with HF exposure. The overall sensitivity was 87.2% (i.e., 197 out of 226 total HF approaches triggered rDBS), while a total of 524 stimulations triggered when no HF pellet approaches were observed.

Discussion

Available studies of NAc-region DBS in psychiatric disease reveal inconsistent results in humans, enforcing the need for a richer physiologic understanding of the most disabling symptoms associated with these heterogeneous diseases as well as DBS itself (26, 27). Despite the use of various assays to probe DBS mechanisms, including measurement of molecular and biochemical markers (i.e., c-Fos, glutamine, gamma-aminobutyric acid, dopamine), pharmacologic manipulations, voltammetry, and advanced imaging in humans, the mechanism of DBS modulation of neuronal population activity remains incompletely explained (14, 28–30). To overcome the limits of biochemical and indirect imaging modalities, electrophysiological recordings during DBS have been attempted, but interpretation of endogenous activity is complicated by electrical stimulation artifact (23, 24). Additionally, electrophysiological studies have shown

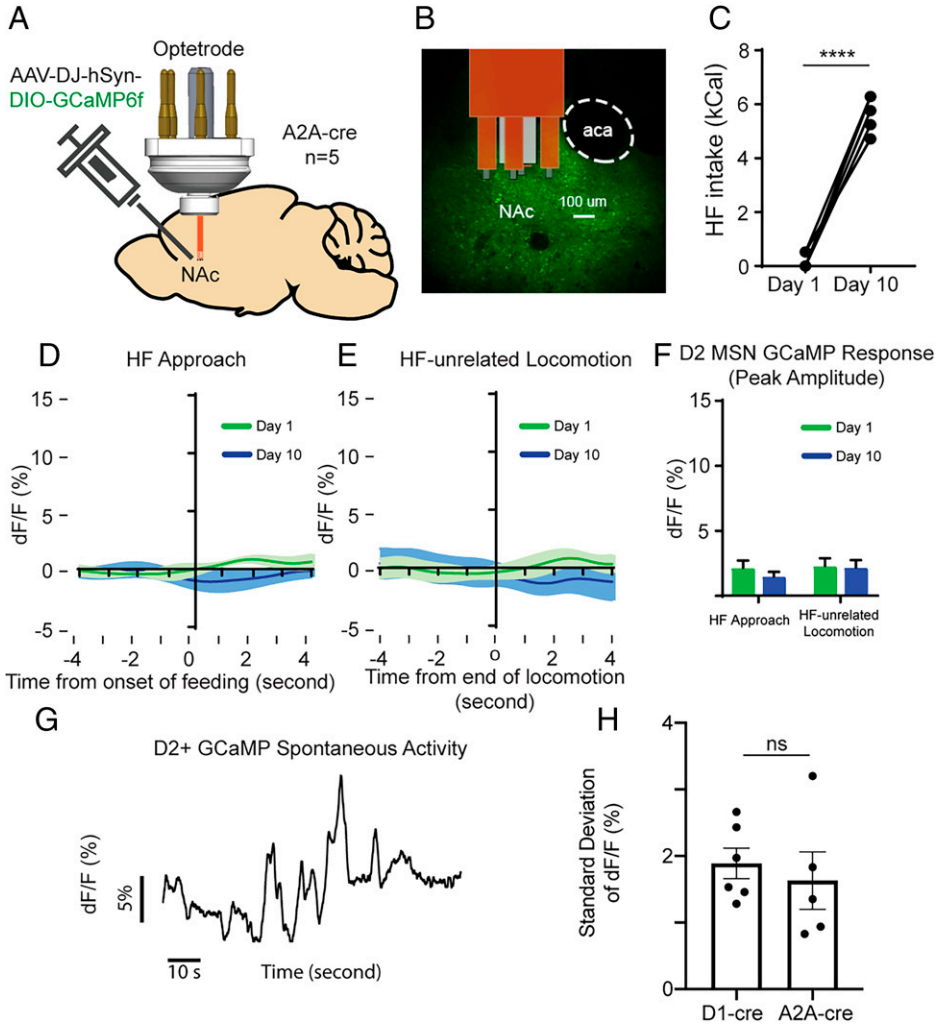

Fig. 3. (*A*) AAV-DJ-hSyn-DIO-GCaMP6f was injected into the NAc in A2A-cre mice, followed by implantation of an optetrode, to allow for measurement of GCaMP6f signals in D2 MSNs. (*B*) Representative image of GCaMP6f expression in D2 MSNs and the optetrode implant in the NAc. (*C*) Hedonic feeding behavior developed and stabilized by day 10 (1 h/d), indicated by a significant increase in daily HF intake. (*D–F*) Average traces and quantification of the peak amplitude of the GCaMP signal from D2 MSNs in the NAc in the 8-s window during HF approach and locomotion unrelated to HF food on days 1 and 10. (*G*) Representative spontaneous GCaMP fluorescence from D2 MSNs. (*H*) SD of GCaMP fluorescence of D1 and D2 MSNs during 5 min of the off-stimulation period. Data represent mean ± SEM. ****$P < 0.0001$. ns, nonsignificant, $P > 0.05$.

disparate findings of both neuronal activation and suppression dependent on the neuronal recording site and orientation of the recording probe with respect to local neuronal cell bodies and axons (31). Here, we leveraged prior demonstrations of NAc DBS ameliorating hedonic feeding behavior in mice combined with a methodology capable of assaying the aggregate local activity on physiologic timescales to provide a readout of local DBS effects. While both continuous and responsive DBS strategies induced a surge in GCaMP signal presumably interfering with HF food–related transients, cDBS-related GCaMP signal enhancement decayed over time. This effect was met with a reemergence of the HF food–related NAc activity and increased consumption based on overall HF intake during the intervention. In contrast, rDBS consistently enhanced the GCaMP signal and ameliorated hedonic feeding behavior. Our findings are suggestive not only that continuous stimulation may not be necessary but that it might even be counterproductive.

Specifically, fiber photometry was used to provide an in vivo readout of calcium signals as surrogates for neuronal action potentials in the NAc. Here, GCaMP signal in the NAc of mice exhibiting hedonic feeding behavior was characterized by a gradual increase in the GCaMP signal or "ramping" activity in anticipation of HF intake. Similar ramping activity has been characterized in the dorsal striatum of mice prior to consummatory events and even during events where food reward was expected but not received (32). In our case, during initial exposure to HF food on day 1, the difference between NAc activity (collectively or at D1 or D2 MSNs) during HF approach versus baseline was undetectable. However, after 10 d of limited HF exposure, once hedonic feeding was induced in these same mice, there was a robust activation of the NAc (primarily in D1 MSNs) during HF approach that paralleled an increase in HF consumption. Interestingly, while we observed increased calcium signaling that potentially correlates with increased neuronal activity, O'Connor et al. reported decreased putative D1-MSN neuronal firing during food consumption (13). These differences may highlight methodological and physiologic differences attributable to the inherent nature of consumption, environment during consumption, and chronic versus acute exposure to a palatable substance. First, the assays used to measure neuronal activity (calcium signal here vs. action potentials) are not directly comparable as detailed in our limitations. Second, here, sated mice had exhibited hedonic feeding previously reported to be associated with altered networks involving

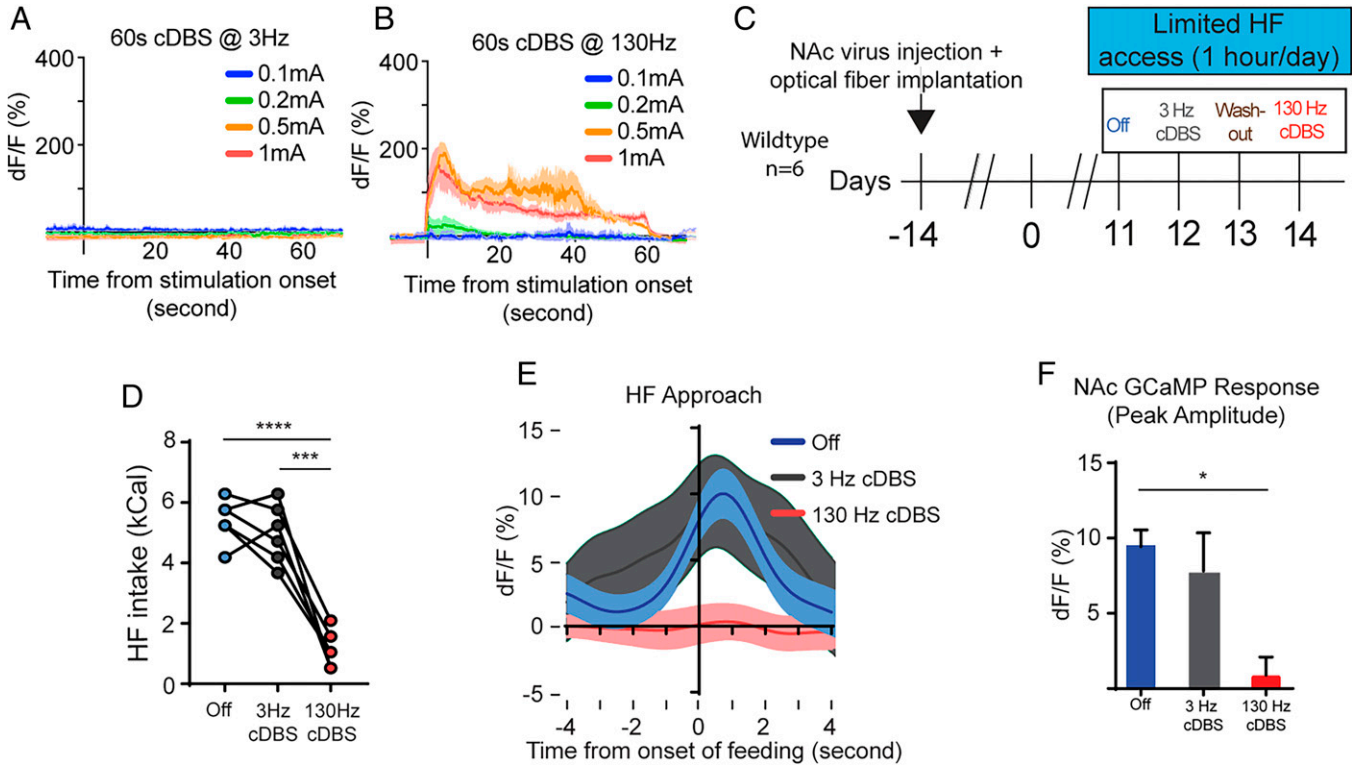

Fig. 4. NAc GCaMP response to open-loop or cDBS. (*A* and *B*) Average GCaMP fluorescence response with cDBS at 3 Hz (*A*) and 130 Hz (*B*), at 0.1, 0.2, 0.5, and 1.0 mA. (*C*) Schematic of the experimental design: virus injection and electrode implantation, followed by a recovery period (14 d), limited HF food access (days 1 to 10), and various paradigms of electrical stimulation. (*D–F*) Behavioral (*D*) and GCaMP (*E* and *F*) response to off- and 3- and 130-Hz cDBS. Data represent mean ± SEM. **P* < 0.05, ****P* < 0.001, *****P* < 0.0001.

the NAc after limited HF food exposure (33) and, therefore, differences in reported neuronal responses may reflect altered neuronal network dynamics (34). Furthermore, other studies have reported results opposite that of the O'Connor et al. paper, that D1-MSN activation increased, whereas inhibition decreased, food intake (35) or that D1-MSN inhibition decreased the breakpoint for a food reward, albeit also in food-deprived mice (36). Additionally, our prior work has highlighted the contribution of D2 receptor–expressing neurons in the mechanism of hedonic feeding using nontarget-specific pharmacologic blockade as an assay (14). Involvement of D2 receptor–expressing neurons (and possibly D2 MSNs) certainly does not exclude possible effects on D1 MSNs that could not be directly assayed using the techniques in our prior work. Lastly, pharmacologic blockade of neurons and direct inhibition or decreased signal from calcium imaging using optogenetics or fiber photometry, respectively, are not entirely analogous readouts.

Our results support the hypothesis that DBS may ameliorate overeating behaviors via blunting HF-linked local activity. As we have previously observed, NAc cDBS blocked hedonic feeding behavior (14, 19), and this effect was associated with dampening of NAc activity to its prefeed baseline. When cDBS was delivered for 3 h, however, NAc activity partially reinstated during the measured time window, as did hedonic feeding behavior as measured by videoed HF approaches. Interestingly, both high-frequency cDBS (within the first 10 s) and rDBS exhibited robust and immediate surges (>200% increase in d*F*/*F*) in NAc activity at the moment of initiation that coincided with subsequent hedonic feeding blockade. Prior studies have reported similar robust surges with both electrical and pharmacologic stimulation (37, 38).

Our results suggest that there is a strategy-dependent (i.e., continuous vs. responsive) dissociation in neural activity patterns for DBS. cDBS only initially induced a surge in NAc activity that quickly receded and appeared to disrupt further HF-linked activity at least in the "short term." In contrast, rDBS guided by the delta-band power fluctuations resulted in intermittent surges of GCaMP activity within the NAc that, when delivered beyond the duration of HF exposure, maintained efficacy unlike cDBS. This suggests that stimulating the NAc with either DBS strategy can result in amelioration of hedonic feeding behavior, at least in part through D1-MSN modulation. While the present study cannot completely elucidate a dissociation in the underlying network mechanisms between DBS strategies, intermittent delivery of brief stimulation bouts guided by behaviorally relevant physiology appears to have more durable effects locally within the NAc and behaviorally than one that is continuous. Further, rDBS was effective even while delivering a significantly lower stimulation load. Both cDBS and rDBS in the NAc ameliorate hedonic feeding behavior without impacting overall locomotion or inducing place preference (14, 18, 19). However, NAc cDBS, but not rDBS, reduces novel juvenile interaction time, a validated assay of an appetitive experience in mice (14, 18, 19). Thus, delivering DBS responsively may improve behavioral specificity of this intervention, not to mention durability, and avoid unwanted side effects. Taken together, these experiments support advancing rDBS, a promising intervention of choice for overeating behavior, and provide a physiologic readout of DBS that provides insight into the intervention's role. Of note, while calcium signals have been used to infer neuronal action potential rate, calcium signals are not equivalent to action potentials. The few prior studies in dopaminergic cells inferring spike activity from calcium signals (39) have been limited to ex vivo assessments using single-cell recordings, and therefore their conclusion may not apply when comparing our results with that of O'Connor

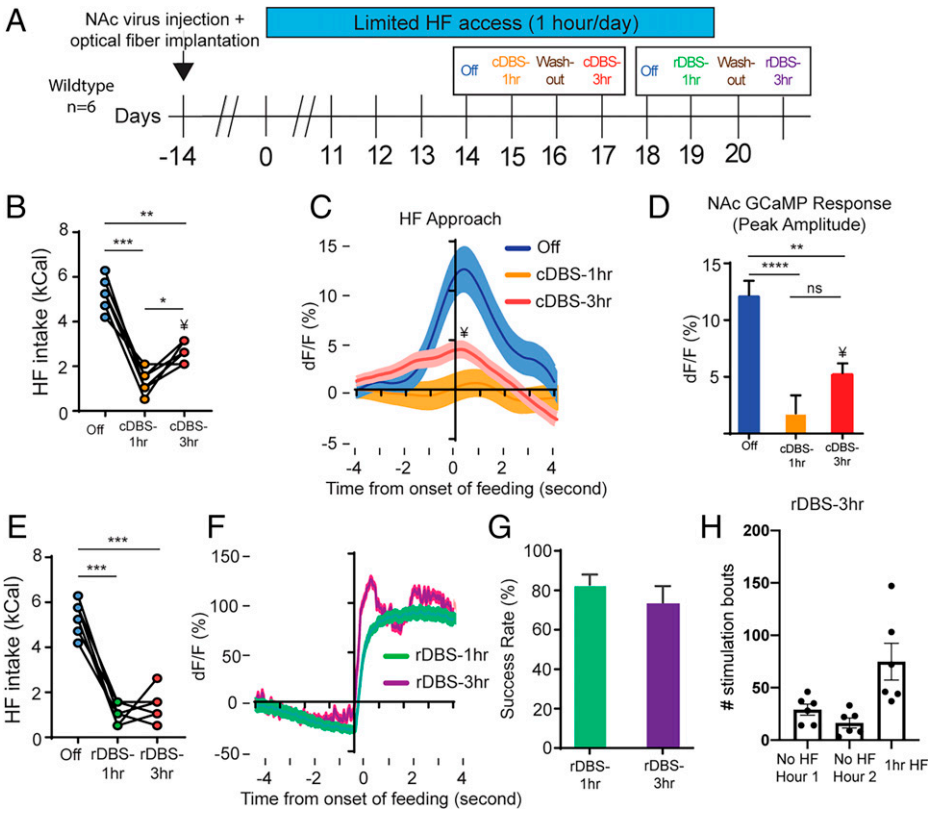

Fig. 5. (*A*) Schematic of the experimental design: virus injection and electrode implantation, followed by a recovery period (14 d), limited HF food access (days 1 to 10), and various paradigms of electrical stimulation. (*B–D*) Behavioral and GCaMP response to open-loop or cDBS applied immediately (cDBS-1h) and 3 h prior to and during (cDBS-3h) exposure to HF food. Time 0 in *C* represents feeding onset. (*E* and *F*) Behavioral and GCaMP response to closed-loop or rDBS applied immediately before (rDBS-1h) and 3 h prior to (rDBS-3h) exposure to HF food. Time 0 in *F* represents stimulation onset. (*G*) Success rates of rDBS-1h and rDBS-3h to block hedonic feeding behavior during limited HF food exposure. (*H*) The number of rDBS stimulation bouts during the 1-h HF exposure and 3-h prior without HF exposure are 74.83 ± 17.53 and 45.33 ± 9.83, respectively (29.00 ± 5.29 and 16.33 ± 4.67 for first and second hours without HF exposure, respectively). Data represent mean ± SEM. $*P < 0.05$, $**P < 0.01$, $***P < 0.001$, $****P < 0.0001$. ns, nonsignificant, $P > 0.05$. ¥, partial reinstatement of HF intake and calcium signal with cDBS-3h.

et al. (13). Further, calcium signaling is not exclusive to action potentials and may be activated by subthreshold depolarization and capture intrinsic, input, and output activity. Therefore, population calcium signal changes as measured here may not directly reflect action potential activity. While we observed D1-MSN activity and feeding changes with NAc stimulation, we are unable to make conclusions on causation using DBS due to its nonspecific, cell-type effects. We cannot exclude influence of DBS on fibers of passage nor antidromic effects. As we are only measuring locally, it is certainly possible, however, that cDBS and rDBS have different effects on the overall network implicated by stimulating the NAc electrically. Here, we limited the "long-term" duration of cDBS to a 3-h period, as a loss of hedonic feeding blockade was seen precluding the need to test longer periods. We did not examine longer-term exposures to HF food as we stimulated outside of the 1-h protocol, given the importance of maintaining stable hedonic feeding levels with limited HF exposures (40). We also only tested rDBS parameters previously used in mice. Undoubtedly, further work is needed to increase our understanding of the GCaMP fluorescence signal captured from the NAc and how it may be altered by electrical stimulation, and to optimize the behavioral specificity of rDBS. While the stereotactic coordinates used were specific to the NAc shell subregion, we do not anticipate that the calcium imaging or DBS effects were entirely subregion-specific. DBS induces a nonphysiologic state that likely has broad effects not specific to one cell type that may also change the relationship between neuronal activity, calcium concentration dynamics, and GCaMP fluorescence. Further, the NAc acts within a larger corticostriatal network to modulate behavior, and assaying responses from additional nodes in this network could help further ascertain the specificity of the reported changes.

Using in vivo calcium imaging, we have revealed intriguing effects on the NAc neural activity associated with DBS-induced behavioral alterations. Implementation of this unique combinatorial methodology to better understand mechanisms of these and other forms of neuromodulation for various indications may help advance the field to identify novel therapies and their targets with applications extending beyond obesity.

Methods and Materials

Wild-type C57BL/6J mice (8 wk) were purchased from The Jackson Laboratory, and Drd1-cre and A2a-cre mice (8 wk) were bred in-house (41, 42). The A2A-Cre line allows for more specific targeting of D2 MSNs which are enriched in A2A receptors (43). Mice were individually housed on a 12-h light/dark schedule (food and water ad libitum). Group housing of mice for feeding experiments such as this can confound overall consumption of each independent mouse and lead to inconsistent intake. We use this behavioral model with independent housing as the mice then tend to consume a stable amount once hedonic feeding behavior has developed. This makes the baseline consumption stable such that we can then interpret a stimulated response. House chow contained 18.6% protein, 44.2% carbohydrates, and 6.2% fat by calories and 3.10 kcal/g (Teklad Diet). A very high fat diet, which contained 20% protein,

20% carbohydrates, and 60% fat by calories and 5.24 kcal/g (Research Diets), was used in this study to model hedonic feeding behavior in mice. All procedures conformed to the *Guide for the Care and Use of Laboratory Animals* (44) and were approved by the Stanford University Administrative Panel on Laboratory Animal Care (APLAC-30216).

Viral Construct, Surgery, and Histology. After 1 wk of habituation, mice were anesthetized with ketamine/xylazine and mounted in a stereotaxic frame (Kopf Instruments). Three hundred nanoliters of concentrated virus was injected using a syringe pump (Harvard Apparatus) at 150 nL/min with an oil-filled glass micropipette (diameter 50 μm). Viral titers (AAV-DJ serotype) ranged from 10^{12} to 10^{13} gc/m. For the NAc cell-body imaging experiments, AAV-DJ-hSyn-GCaMP6f and AAV-DJ-Ef1a-DIO-GCaMP6f (from the Stanford vector core) were delivered into the left NAc (relative to bregma: 1.34 mm anterior, 0.60 mm lateral, and 4.25 mm ventral to the brain surface) in 8-wk-old wild-type C57BL/6J ($n = 6$), and Drd1-cre ($n = 6$) and A2a-cre mice ($n = 6$). Ten minutes later, an optical fiber (400/430 μm, 0.66 numerical aperture; Doric Lenses) or an optetrode, which consisted of the optical fiber surrounded by four PtIr tetrode wires (70/30% Pt/Ir, 100/140 μm, 20 ± 5 kOhm; Doric Lenses) mounted into a microdrive assembly, was implanted into the left NAc (relative to bregma: 1.34 mm anterior, 0.60 mm lateral, and 4.15 mm ventral to the brain surface) (45). This region of the NAc is considered the shell subregion, though it is possible that our recordings and stimulation effects may at least in part encompass the core, and thus we do not specify subregion in the manuscript. Behavioral training commenced 2 wk following surgery. Meloxicam (a nonsteroidal antiinflammatory drug) was used for postoperative pain management.

At the end of the behavioral protocol, mice were anesthetized with pentobarbital and perfused transcardially with 4% paraformaldehyde fixative. Electrodes then were removed. Whole brains were extracted from the crania, postfixed for 24 h, and submerged in phosphate-buffered saline for 48 h. Brains were sliced by microtome into 60-μm coronal sections and mounted on slides with MOWIOL plus DAPI solution and examined under a confocal microscope to verify implant placement.

Behavioral Testing. To induce hedonic feeding behavior, mice were put on a limited HF food exposure protocol (1 h/d) (14, 40). This protocol is known to induce binge-like eating behavior in noncalorically restricted C57BL/6J mice (chow ad libitum) because of the brevity and intermittent nature of the exposure (14, 40). Briefly, a single, preweighed HF food pellet (20% protein, 20% carbohydrates, and 60% fat by calories and 5.24 kcal/g; Research Diets) was provided to the mice in their home cage daily at a fixed time for 1 h. Mice had 24-h access to chow during these periods. Intake of the HF diet within that 1-h period was measured. All mice developed stable (<10% variation across 3 consecutive days) hedonic feeding (defined as 25% of a mouse's daily caloric intake within a 1-h period during the light cycle) after 10 consecutive days on the limited HF food exposure protocol. This behavior was measured during the light cycle when mice do not typically consume most of their calories.

Video recordings were performed for offline analysis. Time frames were extracted from the video for when the mouse approached HF food (referred to as the "HF approach") or had locomotion that ended without approaching HF food, for example, walking from one corner to another corner of the cage where there was no HF food interaction involved (movement unrelated to HF).

GCaMP Photometry Recordings. Fiber photometry data were acquired with Synapse software controlling an RZ5P lock-in amplifier (Tucker-Davis Technologies). A frequency-modulated 473- and 405-nm light-emitting diode (Doric) was used to stimulate calcium ion–dependent and isosbestic emission, respectively (band pass–filtered with Fluorescence Mini Cube FMC4 [Doric], emission was measured with a femtowatt photoreceiver [2151; Newport], and signal was digitized at 6 kHz). To remove motion artifact and fluorescence bleaching, the calcium-insensitive signal ($F405$) was subtracted from the calcium-sensitive signal ($F473$), and then divided by its mean value to obtain the fractional fluorescence response ($F473 - F405$)/mean ($F405$), GCaMP signal, or dF/F. If fluorescence decay of $F473$ and $F405$ had a nonlinear correlation (i.e., $F473/F405$ was markedly nonlinear), each signal was debleached by fitting with a mono- or biexponential decay function, and the final corrected dF/F was calculated as $dF/F473 - dF/F405$. Video frames were analyzed online and GCaMP signals were acquired (46). Experimental time stamps (e.g., initiation of electrical stimulation) were acquired using TTL pulses generated by the recording apparatus and synchronized with the GCaMP signals (45). To extract hedonic feeding behavior, HF approach, and HF food–unrelated locomotion events, a blinded evaluator (S.N.) manually inspected each video and recorded relevant frames numbers, and a time-locked dF/F response was obtained.

Deep Brain Stimulation. Electrical stimulation was applied continuously to mimic cDBS with stimulation parameters set as 0.1 mA, 130 Hz, bipolar, biphasic, and 90-μs pulse width. For the closed-loop or rDBS strategy, stimulation (0.1 mA, 130 Hz, bipolar, biphasic, and 90-μs pulse width for 10 s) was triggered by a programmable biomarker detector previously defined (Neurostimulator, Model RNS-300; NeuroPace). Low-frequency cDBS (0.1 mA, 3 Hz, bipolar, biphasic, and 90-μs pulse width) was applied as a control. The biomarker detection setup for delta oscillations was as previously described: 1,200-ms window size, count criterion 4, band-pass hysteresis 255, band-pass threshold 3, and 20% increase in delta power (19). Success rate of rDBS was defined as (number of blocked HF approaches)/(number of total HF approaches) × 100 (HF approach was identified in video data blindly).

Statistical Analysis. Student's t test (paired) and one- or two-way ANOVAs were used to determine statistical differences using Prism 7 (GraphPad). Post hoc analyses were corrected using Tukey's range test. Statistical significance: $^{*}P < 0.05$, $^{**}P < 0.01$, $^{***}P < 0.001$, $^{****}P < 0.0001$. All data are presented as mean ± SEM.

Data Availability. All study data are included in the article and/or *SI Appendix*.

ACKNOWLEDGMENTS. This study was supported by funds from K12NS080223 (to C.H.H.), K08MH110610 (to B.D.H.), and K99DK115985 (to D.J.C.), the Brain & Behavior Research Foundation (C.H.H. and D.J.C.), Neurosurgery Research and Education Foundation (C.H.H.), John A. Blume Foundation (C.H.H.), William Randolph Hearst Foundation (C.H.H.), and Stanford Medical Scholars Research Fellowship (C.H.H.), and start-up funds from Stanford's Department of Neurosurgery (to C.H.H.).

1. P. P. J. Hay, J. Bacaltchuk, S. Stefano, P. Kashyap, Psychological treatments for bulimia nervosa and binging. *Cochrane Database Syst. Rev.* **2009**, CD000562 (2009).
2. P. P. J. Hay, A. M. Claudino, M. H. Kaio, Antidepressants versus psychological treatments and their combination for bulimia nervosa. *Cochrane Database Syst. Rev.* **2001**, CD003385 (2001).
3. J. I. Hudson, E. Hiripi, H. G. Pope Jr., R. C. Kessler, The prevalence and correlates of eating disorders in the National Comorbidity Survey Replication. *Biol. Psychiatry* **61**, 348–358 (2007).
4. F. Amianto, L. Ottone, G. Abbate Daga, S. Fassino, Binge-eating disorder diagnosis and treatment: A recap in front of DSM-5. *BMC Psychiatry* **15**, 70 (2015).
5. M. A. White, M. A. Kalarchian, R. M. Masheb, M. D. Marcus, C. M. Grilo, Loss of control over eating predicts outcomes in bariatric surgery patients: A prospective, 24-month follow-up study. *J. Clin. Psychiatry* **71**, 175–184 (2010).
6. D. Le Grange, S. A. Swanson, S. J. Crow, K. R. Merikangas, Eating disorder not otherwise specified presentation in the US population. *Int. J. Eat. Disord.* **45**, 711–718 (2012).

7. Y. Goto, A. A. Grace, Dopaminergic modulation of limbic and cortical drive of nucleus accumbens in goal-directed behavior. *Nat. Neurosci.* **8**, 805–812 (2005).
8. M. F. Oginsky, P. B. Goforth, C. W. Nobile, L. F. Lopez-Santiago, C. R. Ferrario, Eating 'junk-food' produces rapid and long-lasting increases in NAc CP-AMPA receptors: Implications for enhanced cue-induced motivation and food addiction. *Neuropsychopharmacology* **41**, 2977–2986 (2016).
9. A. Ghazizadeh, F. Ambroggi, N. Odean, H. L. Fields, Prefrontal cortex mediates extinction of responding by two distinct neural mechanisms in accumbens shell. *J. Neurosci.* **32**, 726–737 (2012).
10. E. A. Ferenczi *et al.*, Prefrontal cortical regulation of brainwide circuit dynamics and reward-related behavior. *Science* **351**, aac9698 (2016).
11. E. S. Calipari *et al.*, In vivo imaging identifies temporal signature of D1 and D2 medium spiny neurons in cocaine reward. *Proc. Natl. Acad. Sci. U.S.A.* **113**, 2726–2731 (2016).
12. M. K. Lobo *et al.*, Cell type-specific loss of BDNF signaling mimics optogenetic control of cocaine reward. *Science* **330**, 385–390 (2010).
13. E. C. O'Connor *et al.*, Accumbal D1R neurons projecting to lateral hypothalamus authorize feeding. *Neuron* **88**, 553–564 (2015).
14. C. H. Halpern *et al.*, Amelioration of binge eating by nucleus accumbens shell deep brain stimulation in mice involves D2 receptor modulation. *J. Neurosci.* **33**, 7122–7129 (2013).
15. F. M. Vassoler *et al.*, Deep brain stimulation of the nucleus accumbens shell attenuates cocaine reinstatement through local and antidromic activation. *J. Neurosci.* **33**, 14446–14454 (2013).
16. J. A. Wilden *et al.*, Reduced ethanol consumption by alcohol-preferring (P) rats following pharmacological silencing and deep brain stimulation of the nucleus accumbens shell. *J. Neurosurg.* **120**, 997–1005 (2014).
17. U. J. Müller *et al.*, Nucleus accumbens deep brain stimulation for alcohol addiction—Safety and clinical long-term results of a pilot trial. *Pharmacopsychiatry* **49**, 170–173 (2016).
18. A. L. Ho *et al.*, Accumbens coordinated reset stimulation in mice exhibits ameliorating aftereffects on binge alcohol drinking. *Brain Stimul.* **14**, 330–334 (2021).
19. H. Wu *et al.*, Closing the loop on impulsivity via nucleus accumbens delta-band activity in mice and man. *Proc. Natl. Acad. Sci. U.S.A.* **115**, 192–197 (2018).
20. B. Rosin *et al.*, Closed-loop deep brain stimulation is superior in ameliorating parkinsonism. *Neuron* **72**, 370–384 (2011).
21. H. Rhew *et al.*, A fully self-contained logarithmic closed-loop deep brain stimulation SoC with wireless telemetry and wireless power management. *IEEE J. Solid-State Circuits* **49**, 2213–2227 (2014).
22. S. Santaniello, G. Fiengo, L. Glielmo, W. M. Grill, Closed-loop control of deep brain stimulation: A simulation study. *IEEE Trans. Neural Syst. Rehabil. Eng.* **19**, 15–24 (2011).
23. C. C. McIntyre, S. Mori, D. L. Sherman, N. V. Thakor, J. L. Vitek, Electric field and stimulating influence generated by deep brain stimulation of the subthalamic nucleus. *Clin. Neurophysiol.* **115**, 589–595 (2004).
24. J. D. Carlson, D. R. Cleary, J. S. Cetas, M. M. Heinricher, K. J. Burchiel, Deep brain stimulation does not silence neurons in subthalamic nucleus in Parkinson's patients. *J. Neurophysiol.* **103**, 962–967 (2010).
25. L. A. Gunaydin *et al.*, Natural neural projection dynamics underlying social behavior. *Cell* **157**, 1535–1551 (2014).
26. D. D. Dougherty *et al.*, A randomized sham-controlled trial of deep brain stimulation of the ventral capsule/ventral striatum for chronic treatment-resistant depression. *Biol. Psychiatry* **78**, 240–248 (2015).
27. I. O. Bergfeld *et al.*, Deep brain stimulation of the ventral anterior limb of the internal capsule for treatment-resistant depression: A randomized clinical trial. *JAMA Psychiatry* **73**, 456–464 (2016).
28. S. Y. Chang *et al.*, Wireless fast-scan cyclic voltammetry to monitor adenosine in patients with essential tremor during deep brain stimulation. *Mayo Clin. Proc.* **87**, 760–765 (2012).
29. N. Yan *et al.*, High-frequency stimulation of nucleus accumbens changes in dopaminergic reward circuit. *PLoS One* **8**, e79318 (2013).
30. P. Riva-Posse *et al.*, Defining critical white matter pathways mediating successful subcallosal cingulate deep brain stimulation for treatment-resistant depression. *Biol. Psychiatry* **76**, 963–969 (2014).
31. C. C. McIntyre, W. M. Grill, D. L. Sherman, N. V. Thakor, Cellular effects of deep brain stimulation: Model-based analysis of activation and inhibition. *J. Neurophysiol.* **91**, 1457–1469 (2004).
32. T. D. London *et al.*, Coordinated ramping of dorsal striatal pathways preceding food approach and consumption. *J. Neurosci.* **38**, 3547–3558 (2018).
33. D. J. Christoffel *et al.*, Input-specific modulation of murine nucleus accumbens differentially regulates hedonic feeding. *Nat. Commun.* **12**, 2135 (2021).
34. K. D. Carr, Nucleus accumbens AMPA receptor trafficking upregulated by food restriction: An unintended target for drugs of abuse and forbidden foods. *Curr. Opin. Behav. Sci.* **9**, 32–39 (2016).
35. X. Zhu, D. Ottenheimer, R. J. DiLeone, Activity of D1/2 receptor expressing neurons in the nucleus accumbens regulates running, locomotion, and food intake. *Front. Behav. Neurosci.* **10**, 66 (2016).
36. A. Natsubori *et al.*, Ventrolateral striatal medium spiny neurons positively regulate food-incentive, goal-directed behavior independently of D1 and D2 selectivity. *J. Neurosci.* **37**, 2723–2733 (2017).
37. G. Schmunk *et al.*, High-throughput screen detects calcium signaling dysfunction in typical sporadic autism spectrum disorder. *Sci. Rep.* **7**, 40740 (2017).
38. H. A. Zariwala *et al.*, A Cre-dependent GCaMP3 reporter mouse for neuronal imaging in vivo. *J. Neurosci.* **32**, 3131–3141 (2012).
39. W. Fleming, S. Jewell, B. Engelhard, D. M. Witten, I. B. Witten, Inferring spikes from calcium imaging in dopamine neurons. *PLoS One* **16**, e0252345 (2021).
40. D. E. Pankevich, S. L. Teegarden, A. D. Hedin, C. L. Jensen, T. L. Bale, Caloric restriction experience reprograms stress and orexigenic pathways and promotes binge eating. *J. Neurosci.* **30**, 16399–16407 (2010).
41. T. Lemberger *et al.*, Expression of Cre recombinase in dopaminoceptive neurons. *BMC Neurosci.* **8**, 4 (2007).
42. S. Gong *et al.*, Targeting Cre recombinase to specific neuron populations with bacterial artificial chromosome constructs. *J. Neurosci.* **27**, 9817–9823 (2007).
43. M. K. Lobo, S. L. Karsten, M. Gray, D. H. Geschwind, X. W. Yang, FACS-array profiling of striatal projection neuron subtypes in juvenile and adult mouse brains. *Nat. Neurosci.* **9**, 443–452 (2006).
44. National Research Council, *Guide for the Care and Use of Laboratory Animals* (National Academies Press, Washington, DC, ed. 8, 2011).
45. C. K. Kim *et al.*, Simultaneous fast measurement of circuit dynamics at multiple sites across the mammalian brain. *Nat. Methods* **13**, 325–328 (2016).
46. B. D. Heifets *et al.*, Distinct neural mechanisms for the prosocial and rewarding properties of MDMA. *Sci. Transl. Med.* **11**, eaaw6435 (2019).